Mon. Not. R. Astron. Soc. **367,** 1594–1602 (2006) doi:10.1111/j.1365-2966.2006.10069.x

Magnetar giant flares and afterglows as relativistic magnetized explosions

Maxim Lyutikov[1,2]★

[1]*University of British Columbia, 6224 Agricultural Road, Vancouver, BC V6T 1Z1, Canada*
[2]*Department of Physics and Astronomy, University of Rochester, Bausch and Lomb Hall, PO Box 270171, 600 Wilson Boulevard, Rochester, NY 14627-0171, USA*

Accepted 2006 January 9. Received 2006 January 7; in original form 2005 November 25

ABSTRACT

We propose that giant flares on soft γ-ray repeaters produce relativistic, strongly magnetized, weakly baryon-loaded magnetic clouds, somewhat analogous to solar coronal mass ejection (CME) events. The flares are driven by unwinding of the internal non-potential magnetic field which leads to a slow build-up of magnetic energy outside of the neutron star. For large magnetospheric currents, corresponding to a large twist of the external magnetic field, the magnetosphere becomes dynamically unstable on the Alfvén crossing time-scale of the inner magnetosphere, $t_{\rm A} \sim R_{\rm NS}/c \sim 30\,\mu$s. The dynamic instability leads to the formation of dissipative current sheets through the development of a tearing mode. The released magnetic energy results in the formation of a strongly magnetized, pair-loaded, quasi-spherically expanding flux rope, topologically connected by the magnetic field to the neutron star during the prompt flare emission. The expansion reaches large Lorentz factors, $\Gamma \sim 10$–20, at distances $r \sim 1$–2×10^7 cm, where a leptophotonic load is lost. Beyond this radius plasma is strongly dominated by the magnetic field, though some baryon loading, with $M \ll E/c^2$, by ablated neutron star material may occur. Magnetic stresses of the tied flux rope lead to a late collimation of the expansion, on time-scales longer than the giant flare duration. Relativistic bulk motion of the expanding magnetic cloud, directed at an angle $\theta \sim 135^\circ$ to the line of sight (away from the observer), results in a strongly non-spherical forward shock with observed non-relativistic apparent expansion and bulk motion velocities $\beta_{\rm app} \sim \cot\theta/2 \sim 0.4$ at times of the first radio observations, approximately one week after the burst. An interaction with a shell of wind-shocked interstellar medium (ISM) and then with the unshocked ISM leads to a deceleration, to non-relativistic velocities approximately one month after the flare.

Key words: stars: individual: SGR 1806-20 – stars: magnetic field – stars: neutron – X-rays: stars.

1 INTRODUCTION

Magnetar emission (see e.g. Woods & Thompson 2004 for a review) is powered by the dissipation of a non-potential (current-carrying) magnetic field (Thompson, Lyutikov & Kulkarni 2002). A dynamo mechanism operating at the birth of neutron stars creates a tangled magnetic field inside a neutron star, which is prevented from unwinding by the rigidity of the crust. The current-carrying plasma exerts the Lorentz force on the crust, which is mostly balanced by the lattice strain. For strong enough magnetic fields, the Lorentz force may induce a stress that exceeds the critical stress of the lattice. This leads to a crustal motion, which should occur along equipotential surfaces: the crust will be rotating. The crustal rotation and the associated twist of the magnetic field lead to the expulsion of the electric current from inside of the neutron star into magnetosphere. The dissipation of magnetospheric currents is responsible for persistent emission (Thompson et al. 2002), while a sudden reconfiguration of a magnetic field may produce flares (Lyutikov 2003). The giant flare of the soft γ-ray repeater (SGR) SGR 1806-20 on 2004 December 27 (we will refer to it as 'the GF') puts new constraints on the model that we discuss in this paper.

★E-mail: lyutikov@phas.ubc.ca

2 WHERE WAS ENERGY STORED RIGHT BEFORE THE FLARE? – IN THE MAGNETOSPHERE

2.1 Short rise time

GFs are powered by dissipation of magnetic field energy. One of the principal issues is where most of the magnetic energy has been stored prior to the GF: in the magnetosphere or in the neutron star crust. These two possibilities are related to two models of GFs of the SGRs. First, a GF may result from a *sudden* untwisting of the

internal magnetic field (Thompson & Duncan 1995, 2001, hereafter TD95 and TD01, respectively). In this case, a large and quick (on the time-scale of a flare) rotational displacement of the crust leads to *an increased twisting of magnetospheric magnetic field lines*. Alternatively, a *slow* untwisting of the internal magnetic field leads to a gradual twisting of magnetospheric field lines, on time-scales much longer than the GF, until it reaches a dynamical stability threshold due to increasing energy associated with the current-carrying magnetic field. Then a *sudden relaxation* of the twist outside the star and the associated dissipation and magnetic topology change lead to flares, in analogy with solar flares and coronal mass ejections (CMEs). Note that even in the case of crustal storage of magnetic field energy before the flare (TD95; TD01), dissipation also occurs in the magnetosphere, not in the crust.

The best test of these two alternatives is the time-scale for the development of a flare. Since energy involved in the GF requires that a large fraction of the magnetosphere is affected, the typical size of the active region is of the order of the neutron star radius. A sudden unwinding of the crust should occur either on the shear wave or Alfvén wave crossing times of the star $t_{\rm A,NS} \sim R_{\rm NS}/V_{\rm s,NS} \sim R_{\rm NS}/V_{\rm A,NS} \sim 0.2$–$0.5$ s (TD95), while magnetospheric instability may develop on time-scales as short as an Alfvén crossing time of the inner magnetosphere, $t_{\rm A,ms} \sim R_{\rm NS}/c \sim 30$ μs (Lyutikov 2003). Observations of the GF made on the December 27 show that it has a very short rise time; ~ 0.25 ms (Palmer et al. 2005). *The very short rise time of the GF points to a magnetospheric origin thereof* (in a sense that right before the flare the energy to be released is stored in the magnetosphere).

2.2 Pre- and post-burst evolution of persistent emission

An *XMM–Newton* observation of SGR 1806-20 months before the GF shows an increased activity, with persistent flux increasing by a factor of 2, spectrum hardening (photon power-law index decreased from 2.2 to 1.5) and spin-down increasing (Mereghetti et al. 2005), all in agreement with the prediction of the twisted magnetosphere model (Thompson et al. 2002), implying an increasing twist before the GF. In addition, two months after the GF, the pulsed fraction and the spin-down rate have significantly decreased and the spectrum has softened (Rea et al. 2005). The same occurred in SGR 1900+14 following the August 27 GF (Woods et al. 2001). All of these effects are consistent with increasing of the twist during the time leading to the GF and decreased twist of external magnetic fields after the GF, brought about by reconnection: (i) in the reconnection model the post-flare magnetosphere is expected to have a simpler structure, as the pre-flare network of currents has been largely dissipated; (ii) the non-thermality of the spectrum is a measure of the current strength in the bulk of magnetosphere (Thompson et al. 2002; Lyutikov & Gavriil 2006) with softer spectra corresponding to a smaller twist; (iii) the spin-down rate depends on the amount of current flowing through open field lines and is smaller for a smaller twist. Note that since open field lines occupy only a small fraction of magnetosphere, the spin-down rate probes the current in a relatively small region which should, on the one hand, correlate with a typical current in the magnetosphere on long time-scales, but on the other hand may show large deviations on short time-scales.

2.3 Ejecta must carry a lot of magnetic field

Magnetospheric storage and release of energy lead to the following consequences. First, it is hard to see how most of the energy released in the magnetosphere can be spent on heating the surface of the neutron star and generating heavy ion-loaded outflows. Secondly, dissipation of the magnetic field cannot create magnetic-field-free plasma: it is likely to be limited to equipartition fields since at this point the induced magnetic field of gyrating relativistic particles will create a magnetic field comparable to the initial field (at temperatures near 500 keV, the energy in photons will be comparable to energy in electrons). Thus, only approximately half of the magnetic field is expected to be converted to particle and photon energy, not much more. Most of the dissipated energy will be later radiated away and/or spent on $p\,{\rm d}V$ work during expansion.

Thus, a magnetospheric release of energy, indicated by very short rise time of the GF, decreasing persistent emission and softer post-flare spectrum, leads to the conclusion that expanding plasma must be strongly magnetically dominated. In this paper, we examine the consequences and consistency of the model based on these premises.

3 OVERVIEW OF THE MODEL

Before discussing various details, let us present a short overview of the model: it qualitatively resembles models of solar flares, with the difference that Sun supports an actively operating dynamo, while in magnetars the dynamo operated only during the birth of a neutron star. The energy that will be released in a GF is initially (at times long before the flare) stored in electric currents flowing inside a neutron star. These currents are generated during the birth of the neutron star and are slowly pushed out into the magnetosphere, gated by *slow, plastic deformations* of the neutron star crust. This creates active magnetospheric regions, in analogy with solar spots. An active region consists of a sheared arcade of magnetic flux and surrounding non-potential magnetic structures. As currents (and with them magnetic energy and helicity) are pushed outside the neutron star, the magnetosphere adjusts slowly to the changing boundary conditions. During this phase, magnetic energy is slowly stored in the magnetosphere. As more current is pushed outside, the magnetosphere reaches a point of dynamical instability beyond which a stable equilibrium cannot be maintained. Crossing the instabilities threshold leads to changing of the magnetic configuration on an Alfvén crossing time-scale, the formation of narrow current sheets and the onset of magnetic dissipation (this process is sometimes called magnetic detonation, e.g. Cowley & Artun 1997). This has two consequences. First, a large amount of magnetic energy is converted into kinetic plasma energy and photons. Secondly, dissipation allows a change in the magnetic topology and leads to the formation of an expanding magnetic loop that eventually breaks away from the star. Initially, after the onset of reconnection, the kinetic pressure of the optically thick pair plasma and magnetic stresses are comparable, so that expansion is quasi-isotropic and reaches relativistic Lorentz factors $\geqslant 10$, determined either by baryon loading or, in the case of very small baryon loading, by the amount of residual pairs.

During the prompt phase of the GF, the expanding magnetic *loop remains attached to the star*; see Fig. 1. The tying of the expanding loop to the star eventually leads to collimation of the explosion into a wide opening angle of the order of 1 sr. After losing the pair load, the expanding cloud is dominated by the magnetic field (magnetic cloud) and eventually disconnects from the neutron star, moving relativistically *away* from the observer at an angle $\sim 135^\circ$. This results in apparent subluminal proper expansion and proper velocity. Eventually, the energy of the magnetic cloud is transferred to the strongly anisotropic forward shock which produces the observed afterglow radio emission.

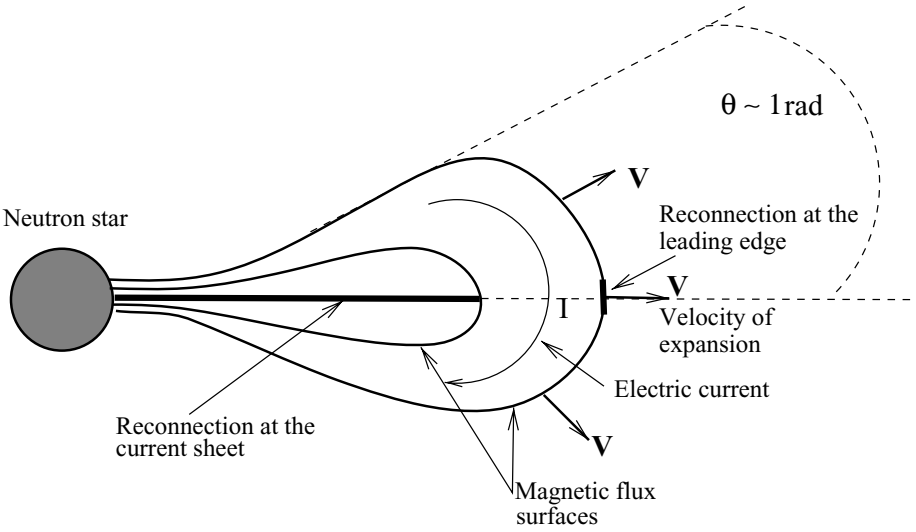

Figure 1. Cartoon of an expanding, collimated flux rope. The twisting of the footpoints of a flux tube leads to electric current flow along the loop and results in its expansion. Beyond some twist angle the dynamic instability leads to formation of dissipative current sheets at the leading edge of the loop, between the footpoints, and possibly in the bulk. Reconnection at the leading edge allows the flux tube to break out of the magnetosphere. Collimating effect of the tied footpoints later leads to broadly collimated outflow.

4 PROMPT AND TAIL EMISSION OF THE GF

4.1 Twisting of the external magnetic field and GF precursors

The central point of our suggestion is that the winding up of external magnetic field proceeds on a long time-scale, much longer than the GF. The winding can occur on time-scale of approximately two months before the GF, indicated by increased activity of the source (Mereghetti et al. 2005). Alternatively, the onset of fairly rapid plastic deformation of the crust may be related to weak emission events (precursors) that seem to precede GFs. [In the case of the GF of SGR 1900+14, a precursor was seen ∼0.4 s before the main burst (Feroci et al. 2001), while in the case of SGR 1806 a relatively powerful event occurs approximately 140 s before the main burst (Palmer et al. 2005).] During the quiescent period between the precursor and the GF, a patch of a crust is continuously rotated by the Lorentz force, balanced both by elastic and viscous stresses in the crust. These two possibilities are not mutually exclusive: slow evolution on a time-scale of months may be followed by a relatively fast twisting over hundreds of seconds before the GF.

Consider a crustal plate of size R rotating under the influence of the Lorentz force, balanced by viscous stresses at the base of the crust. The dissipated power is (Landau & Lifshitz 1975)

$$L_{\rm visc} \sim \frac{4\sqrt{2}\pi^{7/2}\sqrt{\nu}R^4\rho}{T_{\rm rot}^{5/2}} = 1.3\times10^{37}\,{\rm erg\,s^{-1}}\left(\frac{R}{10\,{\rm km}}\right)^4 \times\left(\frac{\rho}{10^{14}\,{\rm g\,cm^{-3}}}\right)\left(\frac{\Delta\phi}{2\pi}\right)^{5/2}, \quad (1)$$

where $\nu \sim 10^4(\rho/10^{14}\,{\rm g\,cm^{-3}})^{5/4}$ is the viscosity of the neutron star (Cutler & Lindblom 1987), ρ is the density at the base of the crust, and $T_{\rm rot} = 140(\Delta\phi)/(2\pi)$ s is the rotation period of the plate, taking into account that instability occurs after rotation of $\Delta\phi$ rad. Total viscously dissipated energy is $E_{\rm vis} \sim L_{\rm visc}T \sim 2\times10^{39}$ erg. [For SGR 1900+14 with $T_{\rm rot} = 0.4$ s, $L_{\rm visc} \sim 3\times10^{43}$ erg s^{-1} and $E_{\rm vis} \sim 10^{44}$ erg, but a very short $T_{\rm rot}$ may indicate that the twist was near critical before the onset of rotation, $\Delta\phi \ll 1$.] Since this energy is released deep in the crust, where the thermal diffusion time to the surface is much longer than $T_{\rm rot}$, most of the heat is absorbed by the core (cf. Lyubarsky, Eichler & Thompson 2002) and does not show as increased persistent emission between the precursor and the main flare.

During plastic creep, the elastic strain is much larger than the plastic strain. The difference between the two can be expressed in terms of how much magnetic field exceeds field at the critical strain:

$$\Delta B \sim 2^{9/4}\pi^{3/4}\sqrt{R\rho}\nu^{1/4}T_{\rm rot}^{-3/4} = 2.7\times10^{10}\,{\rm G}\left(\frac{R}{10\,{\rm km}}\right)^{1/2} \times\left(\frac{\rho}{10^{14}\,{\rm g\,cm^{-3}}}\right)^{1/2}\left(\frac{\Delta\phi}{2\pi}\right)^{3/4} \quad (2)$$

($\Delta B = 2.2\times10^{12}$ G for SGR 1900+14). Thus, during plastic creep only a small fraction of the magnetic energy is dissipated in the crust; most of it is pumped outside of the star.

Note that in the case of the Sun, the *TRACE* satellite has detected a rotation of sunspots associated with the largest (X-class) flares days before the flare (Mewaldt et al. 2005). In addition, solar CMEs also start before the accompanying X-ray flare: there is a quiet growth period of approximately 30 min before the formation of the dissipative current sheet (Zirin 1988).

4.2 During the giant flare the expansion must be relativistic

Relativistic expansion at the time of the GF follows from the conventional compactness argument. For luminosity $L \sim 10^{47}$ erg s^{-1} and variability time-scale ∼1 ms, the optical depth to pair production is (see also Nakar, Piran & Sari 2005)

$$\tau_{\gamma-\gamma} \sim \frac{L\sigma_{\rm T}}{4\pi mc^3R_{\rm NS}} \sim 2\times10^{11}. \quad (3)$$

If plasma were to remain non-relativistic, photon diffusion times would be long, inconsistent with the short observed variability time-scale. This estimate immediately excludes large baryon loading: M must be $\ll E/c^2$. This has always been a standard view of GFs (Feroci et al. 2001; TD01). (A possibility that the initial γ-ray spike

was produced in a relativistic outflow without the dynamically important magnetic field and did not contribute a significant amount of energy to the afterglow is hard to reconcile with the magnetospheric origin.)

At early stages the dissipation of the magnetic field creates an optically dense leptophotonic plasma emerged in the magnetic field with $T \sim (L/4\pi R_{\rm NS}^2\,\sigma_{\rm ST})^{1/4} \sim 300\,{\rm keV}$ (see also Nakar et al. 2005). Qualitatively, the quasi-spherical expansion of a strongly magnetized pair bubble resembles the unmagnetized case, but there are important differences in the asymptotic dynamics (outlined in Appendix A). Initially, plasma expands with the bulk Lorentz factor increasing approximately linearly with radius $\Gamma \propto r$, while the rest temperature decreases $T \sim 1/r$. After reaching $T_\pm \sim 20\,{\rm keV}$ at $r_\pm \sim 1.5 \times 10^7\,{\rm cm}$ (at which point $\Gamma \sim 15$), plasma becomes optically thin. Observed emission is thermal with $T_{\rm obs} = \Gamma T_\pm \sim 300\,{\rm keV}$.

The main implication of relativistic expansion is that outflow is *not* heavily loaded with baryons. In Section 6, we will show that this picture is consistent with the *observed* non-relativistic expansion velocities of the afterglow.

4.3 Initial millisecond spike is nearly isotropic

If the initial spike were strongly anisotropic, with the luminosities inside and outside some emission cone different by orders of magnitude, then we would have observed many more tails without initial spikes. Not a single tail without a spike has been seen. Tails are obviously only weakly anisotropic, emitted by a trapped fireball (TD95), while their intensity is well above the threshold of detectors.

Since the initial γ-ray emission is nearly isotropic, it is unlikely to be produced by a strongly jetted outflow (contrary to Yamazaki et al. 2005). It is still feasible that the initial spike is weakly anisotropic, with radiation intensity and Lorentz factors changing by some factor $\leqslant 2$ depending on direction. [Note that the tail emission in all cases was of the same order, while the energies of the initial spikes were vastly different. This fact is, on one hand, consistent with some structured jetted emission of the initial spike, so that all bursts are the same but the initial spike is viewed from different angles (Yamazaki et al. 2005), but on the other hand it contradicts the fact that the afterglow emission in the case of the GF was several orders brighter, arguing in favour of larger total energetics. Constant tail emission may be explained as a limiting effect of the magnetar magnetic field: above some threshold flare energy, the amount of trapped plasma depends only on the strength of the confining poloidal magnetic field and not on the amount of the released twist.]

4.4 Time-scales of the GF

There are several time-scales in the model: first is the slow initial twist of external magnetic field (Section 4.1). Secondly, there are several time-scales associated with the GF itself: (i) submillisecond initial rise 0.25 ms (ii) $\sim$5 ms rise to the main peak, (iii) hundreds of milliseconds total duration of the spike, (iv) tens of seconds tail emission. Finally, there is an afterglow time-scale of from one week to $\sim$ one month; the latter we identify with non-relativistic transition of the interstellar medium (ISM) blast wave.

Let us discuss the time-scales of the GF itself. Primarily, we associate the shortest time-scale observed in the burst $\sim$0.25 ms with the Alfvén crossing time of the inner magnetosphere. It reflects the dynamical evolution of the magnetosphere after it has crossed the stability threshold. Thus, the very first photons are emitted while the plasma is still not expanding relativistically.

Secondly, since emission requires the dissipation of energy, dissipative time-scales become important as well. In magnetar magnetospheres the development of the dissipative tearing instability occurs on a time-scale that is intermediate between Alfvén time-scales and a resistive time-scale: $t_{\rm tearing} \sim \sqrt{\eta c/R_{\rm NS}}$, where η is plasma resistivity. If resistivity is related to plasma skin depth, $\eta \sim c^2/\omega_{\rm p}$, where $\omega_{\rm p}$ is the plasma frequency, the growth rate of the tearing mode is $\sim$10 ms for a current sheet of width $\sim R_{\rm NS}$ (Lyutikov 2003). The intermediate time-scale $\sim$5 ms observed in the GF may be related to the development of the tearing mode in the current sheets formed during the onset of dynamical instability.

We associate the overall duration of the spike $\sim$100 ms with the dynamical time of the expanding magnetic cloud $\sim 2\,\Gamma^2 c/R_{\rm NS} \sim 25\,{\rm ms}$ for $\Gamma \sim 20$. This is the minimum time it takes for the expanding strongly magnetized bubble to come into causal contact with itself. One expects that on this time-scale the magnetic cloud re-adjusts its internal structure and relaxes to a minimal energy state. This relaxation occurs e.g. through reconnection, which in the relativistic case may proceed with the inflow velocity reaching the velocity of light (Lyutikov & Uzdensky 2003).

Finally, the typical time-scale for the evolution of the tail of the GF, tens of seconds, is well described by radiation leaking from a plasma trapped on closed magnetic field lines (TD95).

4.5 Quasi-thermal spectrum of the initial spike

The thermal spectrum results from radiation escaping from a (strongly magnetized) fireball that becomes optically transparent. An observed temperature of hundreds of keV corresponds to a rest-frame temperature of $\sim$20 keV, when plasma becomes optically thin to pair production, boosted by a Lorentz factor $\sim$10 (Goodman 1986; Paczynski 1986, see also Nakar et al. 2005).

4.6 Mass loading and the terminal Lorentz factor

In Appendix A, we consider the dynamics of a hot, strongly magnetized expanding flow carrying a toroidal magnetic field. The flow is accelerated by magnetic and pressure forces, while both matter inertia and magnetic field energy density provide effective loading of the flow. In addition, in the case of a large-scale magnetic field as considered here, there is an extra conserved quantity: magnetic flux. This plays an important role in the overall dynamics of the flow (cf. Kennel & Coroniti 1984).

If the source luminosity is L, mass loss rate is $\dot{M}_0$ and electromotive force (EMF) is $\mathcal{E}$ (these are conserved quantities), then the terminal Lorentz factor and terminal magnetization parameter σ_∞ are

$$\Gamma_\infty = \frac{L}{\dot{M}_0(1+\sigma_\infty)}, \quad \sigma_\infty = \frac{\mathcal{E}^2}{\Gamma_\infty \beta_\infty \dot{M}_0}, \tag{4}$$

which (formally) expresses the fact that the magnetic field provides additional effective loading (factor $1 + \sigma_\infty$), but the amount of loading depends non-trivially on the parameters of the flow. In the strongly relativistic limit, the outflow typically reaches Alfvén velocity (in fact fast magnetosonic), at which point the Lorentz factor is related to the terminal magnetization parameter as (Goldreich & Julian 1969; Michel 1971)

$$\Gamma_\infty = \sqrt{\sigma_\infty}. \tag{5}$$

To estimate the maximum possible Lorentz factor, we note that the minimum mass loading is determined by residual leftover pairs, determined by equating the annihilation and expansion rates

(Goodman 1986; Paczynski 1986; Nakar et al. 2005)

$$M_{\rm min} = m_{\rm e} N_{\pm} = \frac{4\pi R_0 c t T_0^3 m_{\rm e}}{\sigma_{\rm T} T_{\pm}^3} = 2 \times 10^{17}\,{\rm g}. \quad (6)$$

If most of the energy is in magnetic form, this corresponds to $\sigma_{\rm max} = E/M_{\rm min}c^2 = 4.5 \times 10^7$. The corresponding maximum Lorentz factor is $\Gamma_{\rm max} = \sqrt{\sigma_{\rm max}} = 6.7 \times 10^3$. The lower limit on Γ comes from the observed thermal temperature of the initial spike:

$$\Gamma_{\rm min} \sim \frac{T_{\rm obs}}{T_{\pm}} \sim 10\text{–}20. \quad (7)$$

Thus, the flow must be only weakly polluted by baryons. This picture is in full agreement with TD01. In what follows, we adopt a minimum value of $\Gamma = 10$ for numerical estimates. Then, estimating $E \sim L t_{\rm s}$ and $M \sim \dot{M} t_{\rm s}$ and using equation (5), equation (5) gives

$$M \sim \frac{E}{\Gamma \sigma c^2} = \frac{E}{\Gamma^3 c^2} \sim 10^{22}\,{\rm g}. \quad (8)$$

This is the upper limit on the amount of mass ejected during the GF.

4.7 Plasma physics issues

The proposed model of the GF builds on the models of solar CME and, similarly, has a number of problematic plasma physics issues (see e.g. Priest & Forbes 2002, for review). One is what is known as the Aly–Sturrock paradox (Aly 1984; Sturrock 1991): opening of field lines, which is necessary to generate an outflow, requires an increase in the magnetic energy in the system, while the storage model of CMEs requires the magnetic energy to decrease during the formation of the magnetic cloud. There is a number of ways the Aly–Sturrock paradox can be circumvented, the most important being the magnetic reconnection which can change the topology of the field line.

Another problem is that the injection of current occurs on a finite amount of magnetic flux so that in order to expand, the newly formed magnetic cloud has to break through overlying closed dipolar field lines. This is achieved by reconnection at the null point at the leading edge of the magnetic cloud, cf. the 'magnetic breakout' model of Antiochos, DeVore & Klimchuk (1999). Reconnection transfers the unshared magnetic flux associated with the overlying dipolar field to neighbouring flux tubes, allowing the sheared filament to expand and erupt outward. The rate of reconnecting adjusts so that the radial (as seen from the star) propagation velocity is the Alfvén velocity, which in this case is nearly the velocity of light.

5 RADIO AFTERGLOW: QUALITATIVE DESCRIPTION

5.1 Expansion in SGR wind

As the magnetic cloud expands, it becomes transparent at $r_{\pm}$ and its pair density falls by many orders of magnitude. At this point the magnetic cloud becomes strongly magnetically dominated. Initially the magnetic cloud is topologically connected to the star, but eventually reconnection should happen at the footpoints of the magnetic field lines, disconnecting the magnetic cloud from the star. At this point, the magnetic cloud starts to expand into the pre-existing the SGR wind. It is expected that the SGR wind is strongly relativistic, with Lorentz factors $\gg$10–20. Thus, for intermediate baryon loading (such that the magnetic cloud expands with $\Gamma \sim$ 10–20), the magnetic cloud never overtakes the wind, so that expansion occurs as if in a vacuum. Most of the magnetic energy is concentrated in a shell close to the bubble surface with thickness of the order of $ct_{\rm s} \sim 10^9$ cm, where $t_{\rm s} \sim 100$ ms is the flare duration.

5.2 Apparent constant non-relativistic expansion velocity is due to relativistic strongly anisotropic expansion

Observations of constant expansion velocity from two to five weeks after the burst have been interpreted as evidence in favour of large baryon loading, and, as a consequence, weak relativistic initial expansion velocities (Granot et al. 2006). As we argued above, this cannot be the case due to compactness constraints: the flow must be relativistic with small baryon loading.

Apparent non-relativistic expansion velocity can be due to relativistic anisotropic expansion with little emission within the cone $1/\Gamma$ to the line of sight. If the emitting material is moving relativistically at an angle $\theta \gg 1/\Gamma$, then the apparent expanding velocity is $\beta_{\rm app} = \beta \sin\theta/(1-\beta\cos\theta) \approx \beta \cot\theta/2$. To reproduce the observed $\beta_{\rm app} \sim 0.3$–0.4, it is required that the outflow is directed away from the observer at an angle $\sim 135^\circ$.

We have arrived at a seemingly contradictory picture: initially, during the 0.2-s spike of the GF, the expansion should be nearly isotropic, while at later times, the $\geqslant$1 week expansion is strongly anisotropic. Thus, the magnetic cloud should become strongly anisotropic between 0.2 s and 7 d. It is unlikely that anisotropy is achieved by internal magnetic stresses of the freely expanding magnetic cloud or by the collimating effects of the dipolar magnetic field (Section 5.3). We propose that the expanding magnetic cloud becomes strongly anisotropic due to fact that the magnetic fields of the cloud remain attached to the neutron star during most of the prompt phase. Thus, at these times the magnetic topology of the expanding plasma is that of a flux rope; see Fig. 1.

5.3 Spheromak or flux rope?

Last decade two models were proposed for the structure of interplanetary magnetic clouds ejected from the Sun: a magnetic flux rope and a spheromak. The principal difference between the two is that in the case of the spheromak, the magnetic cloud disconnects from the magnetic field of the Sun at early stages of the ejection and becomes quasi-spherical (e.g. Gibson & Low 1998), while the flux rope remains attached to the Sun for a very long time (even at the orbit of the Earth). The two models lead to very different dynamics of the magnetic clouds. Presently, the spheromak model seems to be inconsistent with data (e.g. Farrugia, Osherovich & Burlaga 1995), while the magnetic flux rope model explains well the internal magnetic structure ejected into interplanetary space (Marubashi 2000).

In the case of the GF, the spheromak model seems to be inconsistent with data for the following reason. As we argued above, the initial explosion should be quasi-isotropic, while at later times it should become strongly anisotropic and one-sided. It is unlikely that relativistic, strongly anisotropic explosions are produced due to collimating effects of the internal magnetic field of the expanding blob which is disconnected from the star: for relativistic expansion the collimation by the internal magnetic field is kinematically suppressed (e.g. Bogovalov 2001), and in any case cannot produce a one-sided explosion. The spheromak also cannot be efficiently collimated by the external dipolar magnetic field, since inside the spheromak the internal kinetic and magnetic pressures scale as $\propto B_{\rm sph}^2 \sim r^{-4}$ ($B_{\rm sph}$ is a typical magnetic field inside the spheromak), while $B_{\rm dipolar}^2 \sim r^{-6}$. Thus, if the plasma to be ejected disconnects from

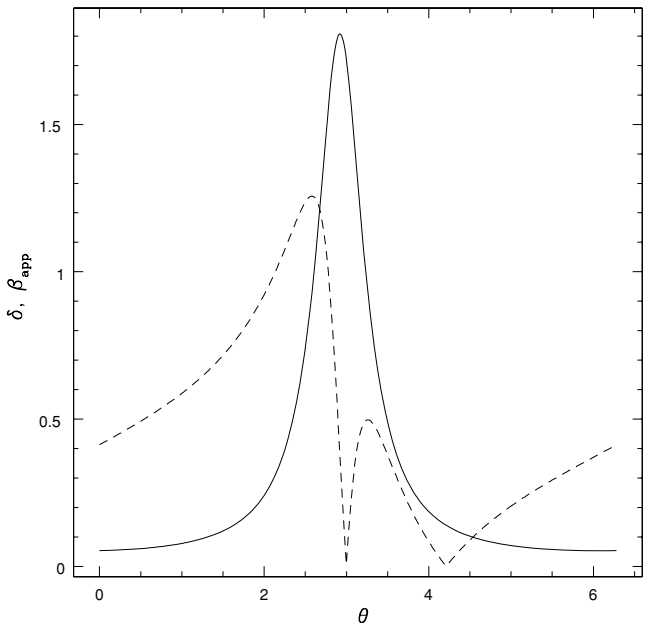

Figure 2. Doppler factor $D = 1/(\Gamma(1 - \beta\cos\theta)$ (solid line) and apparent transverse velocity (dashed line) for a relativistic shock expanding with Lorentz factor $\Gamma = 3$ and moving at $\theta_{\rm ob} = 135^\circ$, with bulk Lorentz factor $\Gamma_{\rm bulk} = 2$, as a function of the angle θ between the explosion direction and the emission point in the rest frame of the explosion for emission points located in the plane containing the direction of the bulk motion and line of sight.

the stellar magnetic field early on, one may expect only weak collimation and, as a result, weak relativistic bulk motion. Since the overall expansion should be strongly relativistic, as we argued in Section 4.2, the observed emission will be dominated by the parts of the shock moving towards the observer, with a somewhat smaller than average Lorentz factor, but having large apparent velocity. To illustrate the point, in Fig. 2, we plot the Doppler factor $\delta = 1/(\Gamma\ (1 - \beta\cos\theta)$ and apparent transverse velocity for a relativistic shock expanding with Lorentz factor $\Gamma = 3$ and moving at $\theta_{\rm ob} = 135^\circ$, with bulk Lorentz factor $\Gamma_{\rm bulk} = 2$, as a function of the angle θ between the explosion direction and emission point in the rest frame of the explosion and the emission points located in the plane containing the direction of the bulk motion and line of sight. Points on the shell with highest Doppler boosting have large apparent transverse velocities, in contradiction with observations.

On the other hand, an expanding magnetic cloud confined by a flux rope (with $B^2_{\rm rope} \sim r^{-4}$) may in principle provide collimation (this would correspond to only regions near $\theta_{\rm ob} \leqslant \pi$ in Fig. 2 contributing to observed emission). Details of this late collimation need to be investigated numerically. From an observational point of view, at late times the expansion should be confined to a fairly broad angle, of the order of π rad, and not to a thin, γ-ray burst-like jet.

6 BASIC AFTERGLOW PARAMETERS

6.1 Geometry

For numerical estimates, we chose $\theta_{\rm ob} = 3\pi/4 = 135^\circ$. Then the apparent velocity $\beta_{\rm app} \sim \beta\cot\theta/2 = 0.41\ \beta$, the Doppler factor $\delta \sim 1/(2\Gamma\sin^2\theta/2) = 0.58/\Gamma$ and the observer time is given by $T = 2r\sin^2\theta/2/(\beta c) = 1.70\, r/(\beta c)$. We assume a strongly magnetized flow with total isotropic energy $E_{\rm ej} \sim 10^{46}$ erg which reaches terminal Lorentz factor $\Gamma = 10$, and is collimated into angle $d\Omega/(4\pi) \sim 0.1$ (so that typical opening angle is $\sim 36^\circ$). We also normalize the surrounding density to $n = 1\,{\rm cm}^3$.

6.2 Typical radii and time-scales

Before the explosion, the magnetar is surrounded by a nearly empty bubble blown by the magnetar wind with a typical size

$$r_{\rm s} \sim \left(\frac{L_{\rm w}}{4\pi n m_{\rm p} c V_{\rm NS}^2}\right)^{1/2} \sim 1.2\times10^{16}\,{\rm cm}\left(\frac{n}{1\,{\rm cm}^{-3}}\right)^{-1/2} \times \left(\frac{V_{\rm NS}}{100\,{\rm km\,s}^{-1}}\right)^{-1}, \quad (9)$$

where $L_{\rm w} \sim 10^{34}\,{\rm erg\,s}^{-1}$ is the average spin-down luminosity of SGR 1806 and $V_{\rm NS}$ is the velocity of the neutron star. Since the magnetar wind is expected to have a Lorentz factor $\Gamma_{\rm w} \gg 10$, until $r_{\rm s}$ the magnetic cloud expands freely, without slowing down. Note that $r_{\rm s}$ is the minimum distance from the neutron star to the shell; depending on the relative orientation of the neutron star velocity and the direction of the explosion, the time when the magnetic cloud overcomes the shell can be larger by a factor of $\sim$2.

Were it to expand in a constant density medium, the flow would starts to decelerate at

$$r_{\rm dec} \sim \left(\frac{3E_{\rm ej}}{d\Omega n m_{\rm p} c^2 \Gamma_0^2}\right)^{1/3} \sim 5.4\times10^{15}\,{\rm cm}\left(\frac{E}{10^{46}\,{\rm erg\,s}^{-1}}\right)^{1/3} \times \left(\frac{n}{1\,{\rm cm}^{-3}}\right)^{-1/3}\left(\frac{\Gamma_0}{10}\right)^{-2/3}. \quad (10)$$

Because $r_{\rm dec} < r_{\rm s}$, the magnetic cloud starts interacting with a shell of shocked ISM plasma at $r \sim r_{\rm s}$. In the observer time this occurs at

$$T \sim 1.7\frac{r_{\rm s}}{c} = 8.2\,{\rm d}. \quad (11)$$

Since the amount of the mass contained in a shell of shocked ISM plasma is $\sim n m_{\rm p} r_{\rm s}^3$, after encountering the shell the Lorentz factor of the magnetic cloud falls to

$$\Gamma \sim \left(\frac{3E}{d\Omega n m_{\rm p} c^2 r_{\rm s}^3}\right)^{1/2} = 2.8\left(\frac{E}{10^{46}\,{\rm erg\,s}^{-1}}\right)^{1/2}\left(\frac{V_{\rm NS}}{100\,{\rm km\,s}^{-1}}\right)^{3/2} \times \left(\frac{n}{1\,{\rm cm}^{-3}}\right)^{1/4}\left(\frac{d\Omega}{0.1\times4\pi}\right)^{-1/2}. \quad (12)$$

The Doppler beaming factor at this point is $\delta = 0.2$.

The transition to the non-relativistic expansion occurs at

$$r_{\rm nr} \sim \left(\frac{3E_{\rm ej}}{d\Omega n m_{\rm p} c^2}\right)^{1/3} \sim 1.7\times10^{16}\,{\rm cm}, \quad (13)$$

corresponding to the observer time

$$T_{\rm nr} = 16.5\,{\rm d}. \quad (14)$$

$T_{\rm nr}$ is an estimate of the time when the velocity of the blast wave starts to deviate considerably from c. It typically takes twice as long for the velocity to fall below $0.5c$, and for the Doppler factor to become within 15 per cent of unity. One expects to see a peak of emission at the moment when Doppler deboosting becomes insignificant, approximately at $\sim 2T_{\rm nr} \sim 33$ d.

6.3 Total energy

From the standard equipartition argument (Pacholczyk 1969), and taking into account Lorentz transformation of flux, $\propto\delta^{3-\alpha}$, and frequency, $\propto\delta$, the minimal energy of relativistic electrons plus magnetic field is

$$E_{\rm min} = 8\times10^{44}\,{\rm erg}\left(\frac{\theta}{65\,{\rm arcsec}}\right)^{9/7} d_{15}^{17/7}\left(\frac{F_\nu}{50\,{\rm mJy}}\right)^{4/7} \times\left(\frac{\nu}{8.5\,{\rm GHz}}\right)^{2/7}\left(\frac{\delta}{0.2}\right)^{-2+4\alpha/7}, \quad (15)$$

where $\alpha\sim0.5$ is the spectral index. This estimate is a factor of $\delta^{-2+4\alpha/7}\sim15$ larger than the one based on the assumption of non-relativistic expansion. The corresponding magnetic field (in the laboratory frame) is

$$B_{\rm min} = 0.1\,{\rm G}\left(\frac{\theta}{65\,{\rm arcsec}}\right)^{-6/7} d_{15}^{-2/7}\left(\frac{F_\nu}{50\,{\rm mJy}}\right)^{2/7} \times\left(\frac{\nu}{8.5\,{\rm GHz}}\right)^{1/7}\left(\frac{\delta}{0.2}\right)^{-1-2\alpha/7}, \quad (16)$$

which is larger by a factor of $\delta^{-1-2\alpha/7}\sim6$ than the one based on the assumption of non-relativistic expansion. Note that the minimal energy argument addresses only the energy in the magnetic field and relativistic electrons. It is expected that most of the energy of the forward shock resides in protons, so that the total energy in the outflow may be order(s) of magnitude larger than (15), bringing it in line with the total energy released in γ-rays.

7 DISCUSSION

In this paper, we outlined a model of a magnetar GF based on the analogy with solar CMEs. Very short rise time-scales of the GF indicate that the GF is driven by the dissipation of energy stored in the magnetosphere right before the burst (as suggested by Lyutikov 2003) and not in the crust of the neutron star (as proposed by TD95). Initially, the explosion is loaded with pairs and is quasi-isotropic. The magnetic field topology of the expanding plasma resembles the flux rope model of CMEs, which leads to late time collimation and anisotropic expansion. The expanding magnetic cloud is strongly dominated by the magnetic field, weakly baryon loaded, with $M\ll E/c^2$, and strongly relativistic. Weeks after the flare, the magnetic cloud still expands relativistically, strongly anisotropically and is moving away from the observer, resulting in apparent expansion velocity $\beta_{\rm app}\sim0.4$. At approximately 33 d, corresponding to a bump in the light curve, the expansion velocity falls below $c/2$. The main prediction of the model is that we may see a medium-energy flare with a very bright radio afterglow, when the explosion will be beamed towards the Earth. Statistically, it should take approximately $\sim1/{\rm d}\Omega\sim10$ GFs.

The magnetospheric dissipation following the plastic deformation of the crust is also consistent with the suggestion of Jones (2003) that neutron star matter cannot exhibit brittle fracture and should instead experience only plastic deformations. On the other hand, the complexity of earthquakes, especially so-called deep focus earthquakes occurring at high pressures, indicates that the Jones (2003) argument is not the end of the story. For example, the crust response may depend on the value of a strain, being plastic at low strains and brittle at high strains (Frohlich 1989).

Can the crustal fractures model be consistent with the above arguments? One possible way is to invoke small-scale ($\sim$100 m) initial crustal deformation (so that the rise time of the GF is short enough), which triggers larger scale deformations in an avalanche-type process (TD95; TD01). In addition, the relatively bright and long-lived afterglow following the August 27 flare is well fitted by the deep crustal heating model (Lyubarsky et al. 2002). The crustal fracture model also has a better chance of explaining post-flare activity (August 27 and March 5 flares followed by a burst-active period) in analogy with earthquake aftershocks.

One possible way to distinguish the models is that the reconnection-type events may be accompanied by coherent radio emission resembling solar type-III radio bursts (Lyutikov 2002). The radio emission should have correlated pulse profiles with X-rays, narrow-band-type radio spectrum with $\Delta\nu\leqslant\nu$ (with the typical frequency $\nu\geqslant1$ GHz), and a drifting central frequency. This requires catching a burst in simultaneous radio and X-ray observations.

ACKNOWLEDGMENTS

We would like to thank Roger Blandford, Yuri Lyubarky and Christofer Thompson for numerous discussions.

REFERENCES

Aly J. J., 1984, ApJ, 283, 349
Antiochos S. K., DeVore C. R., Klimchuk J. A., 1999, ApJ, 510, 485
Bogovalov S., 2001, A&A, 371, 1155
Cowley S. C., Artun M., 1997, Phys. Rep., 283, 185
Cutler C., Lindblom L., 1987, ApJ, 314, 234
Farrugia C. J., Osherovich V. A., Burlaga L. F., 1995, J. Geophys. Res., 100, 12 293
Feroci M., Hurley K., Duncan R. C., Thompson C., 2001, ApJ, 549, 1021
Frohlich C., 1989, Annu. Rev. Earth Planet. Sci., 17, 227
Gibson S. E., Low B. C., 1998, ApJ, 493, 460
Goldreich P., Julian W. H., 1969, ApJ, 157, 869
Goodman J., 1986, ApJ, 308, L47
Granot J. et al., 2006, ApJ, 638, 391
Jones P. B., 2003, ApJ, 595, 342
Kennel C. F., Coroniti F. V., 1984, ApJ, 283, 710
Landau L. D., Lifshitz E. M., 1975, Course of Theoretical Physics, Vol. 4, Fluid Mechanics, 4th edn. Butterworth-Heinemann, Oxford
Lyubarsky Y., Eichler D., Thompson C., 2002, ApJ, 580, 69
Lyutikov M., 2002, ApJ, 580, 65
Lyutikov M., 2003, MNRAS, 346, 540
Lyutikov M., Gavriil F., 2006, MNRAS in press (doi:10.1111/j.1365-2966.2006.10140.x) (astro-ph/0507557)
Lyutikov M., Uzdensky D., 2003, ApJ, 589, 893
Marubashi K., 2000, Adv. Space Res., 26, 55
Mereghetti S. et al., 2005, ApJ, 628, 938
Mewaldt R. A. et al., 2005, in Am. Geophys. Union Fall Meeting 2005
Michel F. C., 1971, Comments Astrophys. Space Phys., 3, 80
Nakar E., Piran T., Sari R., 2005, ApJ, 635, 516
Pacholczyk A. G., 1969, Radio Astrophysics. Freeman & Co., San Francisco
Paczynski B., 1986, ApJ, 308, L43
Palmer D. M. et al., 2005, Nat, 434, 1107
Priest E. R., Forbes T. G., 2002, A&A, 10, 313
Rea N., Tiengo A., Mereghetti S., Israel G. L., Zane S., Turolla R., Stella L., 2005, ApJ, 627, 133
Schwartz S. J. et al., 2005, ApJ, 627, 129
Sturrock P. A., 1991, ApJ, 380, 655
Thompson C., Duncan R. C., 1995, MNRAS, 275, 255 (TD95)
Thompson C., Duncan R. C., 2001, ApJ, 561, 980 (TD01)
Thompson C., Lyutikov M., Kulkarni S. R., 2002, ApJ, 574, 332
Woods P. M., Thompson C., 2006, in Lewin W., van der Klis M., eds, Cambridge Astrophys. Ser. Vol. 39, Compact Stellar X-Ray Sources. Cambridge Univ. Press, Cambridge, in press (astro-ph/0406133)

Woods P. M., Kouveliotou C., Göğüş E., Finger M. H., Swank J., Smith D. A., Hurley K., Thompson C., 2001, ApJ, 552, 748
Yamazaki R., Ioka K., Takahara F., Shibazaki N., 2005, PASJ, 57, 11
Zirin H., 1988, Astrophysics of the Sun. Cambridge Univ. Press, New York

APPENDIX A: DYNAMICS OF MAGNETIZED PAIR-LOADED FLOWS

In this section, we consider the dynamics of a hot relativistic, spherically symmetric, stationary outflow carrying a toroidal magnetic field. Because the energy release during the GF lasts $\sim$0.1 s, on small time-scales and for radii $\leqslant 10^9$ cm, the flow may be considered stationary. In addition, the internal energy density in the expanding magnetic cloud scales more slowly with the radius, $\propto r^{-4}$, than the energy density of the dipolar field, $\propto r^{-6}$, so that dynamical effects of the dipolar magnetic field quickly become negligible. At this stage expansion is quasi-isotropic, as discussed in Section 4.3. The rotation and dynamical effects of the poloidal magnetic field are neglected.

The dynamics of such a warm magnetized wind is controlled by three parameters: energy L, mass flux $\dot{M}$ and the EMF $\mathcal{E}$ produced by the expanding magnetic cloud. The total energy flux may be divided into two forms: mechanical $L_{\rm M}$ and electromagnetic $L_{\rm EM}$ luminosities:

$$L = L_{\rm M} + L_{\rm EM}. \tag{A1}$$

We wish to understand how the parameters of a fully relativistic flow (velocity β, pressure p, magnetization σ) evolve for an arbitrary ratio of both $L_{\rm EM}/L_{\rm M}$ and p/ρ (ρ is the rest-frame mass density).

The asymptotic evolution of the flow is determined by conserved quantities which may be chosen as the total luminosity L, the mass flux $\dot{M}$ and the EMF $\mathcal{E}$. Thus, the central source works both as a thruster and as a dynamo.

The formal treatment of the problem starts with the set of relativistic MHD equations which can be written in terms of conservation laws. In coordinate form and assuming a stationary, radial, spherically symmetric outflow with toroidal magnetic field, relativistic MHD equations give

$$\frac{1}{r^2}\partial_{\rm r}[r^2(w+b^2)\beta\Gamma^2] = 0, \tag{A2}$$

$$\frac{1}{r^2}\partial_{\rm r}\{r^2[(w+b^2)\beta^2\Gamma^2 + (p+b^2/2)]\} - \frac{2p}{r} = 0, \tag{A3}$$

$$\frac{1}{r}\partial_{\rm r}[rb\beta\Gamma] = 0, \tag{A4}$$

$$\frac{1}{r^2}\partial_{\rm r}[r^2\rho\beta\Gamma] = 0. \tag{A5}$$

The above relations can be simplified by defining

$$\begin{aligned} L &= 4\pi r^2\beta\,\Gamma^2\left(b^2 + \frac{\Gamma_{\rm a}}{\Gamma_{\rm a}-1}\,p + \rho\right),\\ \dot{M} &= 4\pi r^2\beta\,\Gamma\,\rho,\\ \mathcal{E} &= 2\sqrt{\pi}r\,\beta\,\Gamma\,b, \end{aligned} \tag{A6}$$

where we assume that fluid is polytropic with adiabatic index $\Gamma_a[w = \rho + (\Gamma_{\rm a}/\,\Gamma_{\rm a} - 1)p]$, and $\mathcal{E}$ is the EMF.

It is convenient to introduce two other parameters: the magnetization parameter σ as the ratio of the rest-frame magnetic and particle energy–density, and a fast magnetosonic wave phase velocity $\beta_{\rm f}$

$$\begin{aligned} \sigma &= \frac{b^2}{w} = \frac{\mathcal{E}^2}{L\beta - \mathcal{E}^2},\\ \beta_{\rm f}^2 &= \frac{\sigma}{1+\sigma} + \frac{\Gamma_{\rm a}p}{(1+\sigma)w} = (\Gamma_{\rm a}-1)\left(1 - \frac{\Gamma\dot{M}}{L}\right) + (2-\Gamma_{\rm a})\frac{\mathcal{E}^2}{L\beta}. \end{aligned} \tag{A7}$$

Using the three conserved quantities L, $\dot{M}$ and $\mathcal{E}$ the evolution equation becomes

$$\frac{1}{2\beta^2\Gamma}\partial_{\rm r}\Gamma = \frac{(\Gamma_{\rm a}-1)\left(\beta L - \beta\Gamma\dot{M} - \mathcal{E}^2\right)}{r\,\left(\beta L(\beta^2 + 1 - \Gamma_{\rm a}) + (\Gamma_{\rm a}-1)\beta\Gamma\dot{M} - (2-\Gamma_{\rm a})\mathcal{E}^2\right)}. \tag{A8}$$

Eliminating $\mathcal{E}$ in favour of $\Gamma_{\rm f}$, we get a particularly transparent form for the evolution of Lorentz factor

$$\frac{\left(\Gamma^2 - \Gamma_{\rm f}^2\right)}{\beta^2\Gamma^3}\partial_{\rm r}\Gamma = \frac{2p\Gamma_{\rm a}}{(w - \Gamma_{\rm a}p)r}. \tag{A9}$$

Equation (A9) is a nozzle-type flow (e.g. Landau & Lifshitz 1975). The left-hand side of equation (A9) contains a familiar critical point at the sonic transition $\Gamma = \Gamma_{\rm f}$. The positively defined right-hand side describes the evolution of Lorentz factors due to kinetic pressure effects. In the case of purely radial expansion the magnetic gradient forces are exactly balanced by the hoop stresses, so that the magnetic field does not contribute to acceleration. From equation (A9), it follows that superfast-magnetosonic flows accelerate while subfast-magnetosonic flows decelerate. It also follows that terminal Lorentz factor of the flow is determined by the condition $\partial_{\rm r}\Gamma = 0$ which implies that either $p = 0$ or $\beta_\infty = 0$. Condition $\beta_\infty = 0$ can be reached only for subsonic flows with $\mathcal{E} = 0$. Neglecting the $\beta_\infty = 0$ solution, the terminal velocity of magnetized flow is determined by the condition

$$L = \Gamma_\infty\dot{M} + \frac{\mathcal{E}^2}{\beta_\infty}. \tag{A10}$$

For each set of parameters (L, $\dot{M}$ and $\mathcal{E}$), there are generally two solutions of equation (A10) for the terminal four-velocity. The only exception is the case of zero magnetization, $\mathcal{E} = 0$, when the terminal (supersonic) Lorentz factor is uniquely determined by $\Gamma_\infty = L/\dot{M}$.

For non-zero magnetization, the terminal velocity cannot be determined uniquely from given L, $\dot{M}$ and $\mathcal{E}$. Solutions exist only for $L/\dot{M}$ larger than some critical value $L/\dot{M} = (1 - (\mathcal{E}^2/L)^{2/3})^{-3/2}$, corresponding to $\beta_\infty = (\mathcal{E}^2/L)^{1/3}$. For fixed $\dot{M}$ and $\mathcal{E}$, the minimum energy loss is reached at $\beta_{\rm min}$. Assumption $\beta_\infty = \beta_{\rm min}$ then gives

$$\left[1 + (\beta_\infty\Gamma_\infty\sigma_\infty)^{2/3}\right]^{3/2} = \frac{\Gamma_\infty\sigma_\infty}{\beta_\infty^2}, \tag{A11}$$

which in the strongly relativistic limit gives the Michel solution

$$\Gamma_\infty = \sqrt{\sigma_\infty}. \tag{A12}$$

We can also relate the terminal magnetization σ_∞ to the magnetization at the source – more specifically, to magnetization at the sonic point $\sigma_{\rm f}$:

$$\sigma_{\rm f} = \begin{cases} \dfrac{\sigma_\infty}{\Gamma_{\rm a}-1} = 3\sigma_\infty & \text{if } \sigma_\infty \ll 1,\\ \dfrac{(4-\Gamma_{\rm a})\sigma_\infty}{2} = \dfrac{4}{3}\sigma_\infty & \text{if } \sigma_\infty \gg 1. \end{cases} \tag{A13}$$

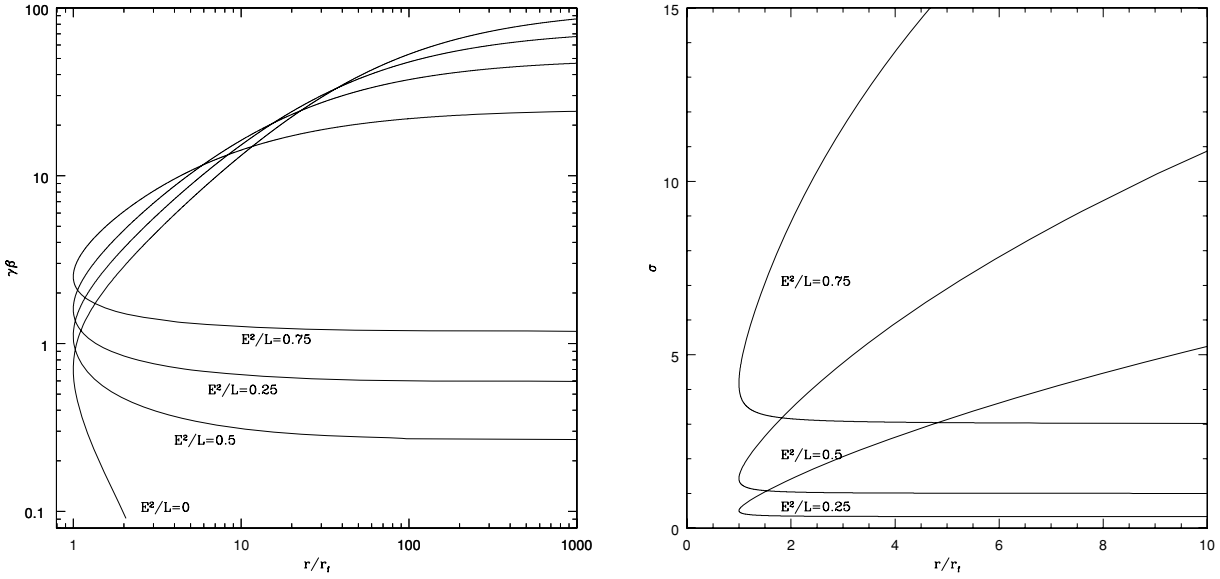

Figure A1. Evolution of strongly magnetized and hot flows. (a) Four velocities of flows are given as functions of $r/r_{\rm f}$ for $L/\dot{M} = 100$ and different values of the parameter E^2/L. Flows start at $r = r_{\rm f}$ with $\beta = \beta_{\rm f}$; supersonic flows first accelerate as $\beta\gamma \sim r$, reaching a terminal value given by the larger root of equation (A10), while subsonic decelerate initially as $\beta \sim r^{-2}$ reaching asymptotic value given by the smaller root of equation (A10). (b) Magnetization parameter σ. For supersonic flows (lower branch), the magnetization remains constant, reaching $\sigma_\infty = (1 - (E^2/L)^{-1})$ as $r \to \infty$. Subsonic flows become strongly magnetized as they expand (upper branch); the magnetization parameter increases $\sigma \sim r^{2/3}$.

Thus, we always have $\sigma_\infty < \sigma_{\rm f}$, but they remain of the same order of magnitude: the magnetization of the flow changes only slightly as the flow propagates away from the launching point to infinity. The reason for constant σ in the supersonic regime is that both in the case $p \gg \rho$ (linear acceleration stage) and $p \ll \rho$ (coasting stage) the plasma and the magnetic field energy densities in the flow change with the same radial dependence ($\sim r^{-4}$ and $\sim r^{-2}$ correspondingly).

For arbitrary flow parameters the evolution equations are integrated numerically (Fig. A1). Given the evolution of the flow and the relation for local σ, we can find the evolution of the magnetization parameter (Fig. A1b).

This paper has been typeset from a TEX/LATEX file prepared by the author.